

## Correlation satellites in the atomic photoelectron spectra of group-IIA and -IIB elements\*

Sefik Süzer, S.-T. Lee, and D. A. Shirley

*Materials and Molecular Research Division and Department of Chemistry, Lawrence Berkeley Laboratory, University of California, Berkeley, California 94720*

(Received 20 January 1976)

Atomic vapors of Ca, Sr, Ba, Zn, Cd, and Hg were studied by photoelectron spectroscopy in a special high-temperature cell using He I (and in some cases Ne I or He II) resonance radiation. In addition to strong lines obtained by photoemission from the nominal  $ns^2 + (n-1)d^{10}ns^2$  configurations, weaker lines were observed that are attributed to admixtures of the configurations  $np^2$ ,  $(n-1)d^2$ , etc. (in group-IIA elements) or  $np^2$ , in group-IIB elements, into the ground state. In the group-IIA cases, the satellite intensities are consistent with expectations based on multiconfiguration Hartree-Fock results. Photoelectron spectroscopy thus appears to provide incisive information about the details of electron correlations in these atoms. Intensity ratios of spin-orbit partners fall near the multiplicity ratios in Zn and Cd, but deviate in Hg due to relativistic effects, in agreement with expectations based on earlier work.

### I. INTRODUCTION

Quantum states of multielectron atoms are commonly labeled by their dominant configurations in one-electron orbital bases. For example, the ground state of the helium atom is designated ( $1s^2$ ;  $^1S$ ), while the group-II elements are described as ( $ns^2$ ;  $^1S$ ) if only the valence electrons are considered. Such a simple description cannot be rigorously correct, of course, because it implicitly neglects electron correlations. Correlations may be treated theoretically by admixing additional configurations of the same symmetry; thus the ground state of calcium would be described by

$$\psi(^1S) = a(4s^2) + b(4p^2) + c(3d^2) + \dots \quad (1)$$

This theoretical approach [configuration interactions (CI's)] is commonly used to carry atomic or molecular calculations beyond the Hartree-Fock limit. The total energy is usually employed as a criterion of quality of the computation.

The experimental situation is much less straightforward. Conventional spectroscopic methods usually involve excitation of an  $N$ -electron (bound) excited state. The selection rules are governed by the total symmetries of both states. Configuration mixing may be manifested as deviations from interval rules, irregularities of intensities, etc., but conventional spectroscopy is not particularly sensitive to details of electron correlation.

Photoelectron spectroscopy provides a relatively direct measure of configuration mixing. A photoelectric transition excites an  $N$ -electron system to an  $N$ -electron final state in which, however, one electron is unbound. Thus a calcium atom in our example would be taken, by photoionization of a valence electron, to a state in  $Ca^+$  plus a

free electron. The total  $N$ -electron final state must have  $^1P$  symmetry. Thus the (dipole) selection rules are as stringent for photoelectron spectroscopy as for conventional spectroscopy, when applied to the total system. However, the  $N$ -electron  $^1P$  state can be made up of any one of a wide variety of states in  $Ca^+$  plus a continuum state of symmetry appropriate to satisfy the selection rules. In particular, any one-electron state in  $Ca^+$  that can be reached by removal of an electron from a basis configuration in Eq. (1) should be reached by photoemission. For example, the  $Ca^+(4p^1; ^2P)$  states are accessible from the  $b(4p^2)$  part of the Ca ground-state wave function in Eq. (1), with the second electron leaving in a continuum  $s$  or  $d$  state. Similarly,  $Ca^+(3d^1; ^2D)$  states are accessible from the  $c(3d^2)$  portion of the Ca ground-state wave function, etc. None of these states could be reached by a one-electron process if the Ca ground state were simply  $4s^2$ ; thus observation of the  $^2P$ ,  $^2D$ , etc. lines gives a measure of the extent to which the  $4p^2$ ,  $3d^2$ , etc. configurations are admixed into the ground state. A rigorous quantitative interpretation would require further theoretical developments to correct for differences in photoelectric cross sections for the different  $nl$  orbitals and for two-electron processes.

In this paper we report experimental photoemission studies of vapors of the group-IIA metals Ca, Sr, and Ba and the group-IIB metals Zn, Cd, and Hg, in which several satellite peaks arising from electron correlation have been observed. We have reported similar results for  $^1Cd$  and  $^2Pb$  earlier, while Berkowitz *et al.*<sup>3</sup> have reported satellite peaks in Hg. The alkaline-earth atoms have been treated theoretically by Kim and Bagus<sup>4</sup> using the multiconfiguration Hartree-Fock method. They found that consider-

able electron correlation must be included to bring the calculated generalized oscillator strengths into agreement with experiment. Their calculations included the configurations  $np^2$  and  $(n-1)d^2$  in the ground states, and they found appreciable mixtures of these configurations. Judging from their results, we would expect to find satellite peaks corresponding to  $np$  and  $(n-1)d$  ionic states in the photoemission spectra of alkaline-earth atoms. Group-IIB atoms would be expected to show similar correlation effects.

In this paper, experimental details are given in Sec. II and results in Sec. III. Section IV A discusses the nature of these satellites and Sec. IV B deals with the relativistic effects on the branching ratios of the spin-orbit components. Conclusions are given in Sec. V.

## II. EXPERIMENTAL

The experiments were carried out in a Perkin-Elmer PS-18 photoelectron spectrometer modified for high-temperature work. The details of the modifications have been reported elsewhere.<sup>2</sup>

The spectrum of Hg was taken at about 55°C and that of Cd at about 290°C using the original heated probe provided with the PS-18 spectrometer. The Cd spectrum reported here is different from that of the earlier work<sup>1</sup> in that digital data acquisition was employed, as described earlier.<sup>2</sup> Zinc was run at 380°C, Ca at 740°C, and Sr at 650°C using our high-temperature cell and He I radiation. Barium spectra were taken at 700°C using both He I and Ne I radiation. The He I spectrum of Ba showed very strong autoionization features, in agreement with results reported by other workers.<sup>5</sup> These features are absent in Ne I spectrum. Because of this phenomenon, we shall report here only the Ne I spectrum of Ba. The He I spectrum will be discussed in a separate paper.

At lower pressure, our He lamp produces sufficient He II radiation (~5% He I) to record the He II spectra of Zn, Cd, and Hg. This was actually done, to see how the relative peak intensities changed with photon energies.

Samples were loaded in air, then introduced into the spectrometer. Oxides, which were invariably present in the samples, did not show up in the spectra because of their low vapor pressures. All samples were 99% pure, and no impurity peaks were found in the spectra except in the case of Sr. The first Sr sample used (from Alfa Inorganics) was stated to be of >99.5% purity and contained ~0.3% Ba. Because of the strong resonant absorption of He I radiation in barium, the Ba peaks showed up in fair intensity in the

Sr spectra. Strontium samples of 99.99% purity (from Orion) were then tried, but without much success, because the Ba peaks gained in intensity as the percentage of Ba increased with time. However, all impurity peaks could be identified by comparison with the He I spectrum of pure Ba; thus they did not affect the interpretation of the Sr spectra.

Samples were heated to an optimum temperature for a count rate of  $2-4 \times 10^3$  counts/sec on the most intense peaks. Then the same spectra were taken at temperatures of  $\pm 30^\circ\text{C}$  from the optimum to differentiate between the inelastic-loss peaks and the real photoionization peaks. Energy calibration was done by introducing Ar (or  $\text{N}_2$ ) and Xe together with the sample in a separate run.

Peak areas were corrected for the change of the spectrometer transmission with electron kinetic energy using the approximate relation  $\Delta E/E = \text{const}$ . All of the observed lines are broad in comparison with the instrumental resolution owing to the effects of charging in or around the ionization region. This also affects the transmission function of the spectrometer, which severely discriminates against the low-energy electrons. No correction was made for this effect or for the inelastic scattering of the electrons owing to a finite sample pressure. The latter was shown to affect the area ratios of peaks at different energies.<sup>6</sup> However, neither of these effects is expected to be very important for high-energy electrons. Hence the area ratios reported for the He II results should be reliable. Those for the low-energy satellites must be regarded as only qualitatively correct.

## III. RESULTS

The He I spectra of Ca and Sr and the Ne I spectrum of Ba are shown in Fig. 1. Peak assignments were done by comparison of their binding energies with optical data.<sup>7</sup> These assignments and derived parameter are set out in Table I.

The spectrum of atomic  $\text{Ca}(4s^2; ^1S)$ , Fig. 1(a), shows one main peak at 6.11 eV, corresponding to the  $\text{Ca}^+(4s; ^2S)$  final state, and four additional peaks at 7.82, 9.24, 12.60, and 13.16 eV, corresponding, respectively, to  $(3d; ^2D_{3/2,5/2})$ ,  $(4p; ^2P_{1/2,3/2})$ ,  $(5s; ^2S_{1/2})$ , and  $(4d; ^2D_{3/2,5/2})$  final states. The peak designated by *I* at 9.04 eV is an inelastic-loss peak, resulting from excitation of the transition  $(4s^2 \rightarrow 4s4p; ^1P_1)$  in neutral Ca by monoenergetic electrons from the  $\text{Ca} \rightarrow \text{Ca}^+(4s)$  transition.

The spectrum of atomic  $\text{Sr}(5s^2; ^1S)$ , Fig. 1(b), again shows one main peak at 5.69 eV, from the  $(5s; ^2S_{1/2})$  final state, and five additional peaks at

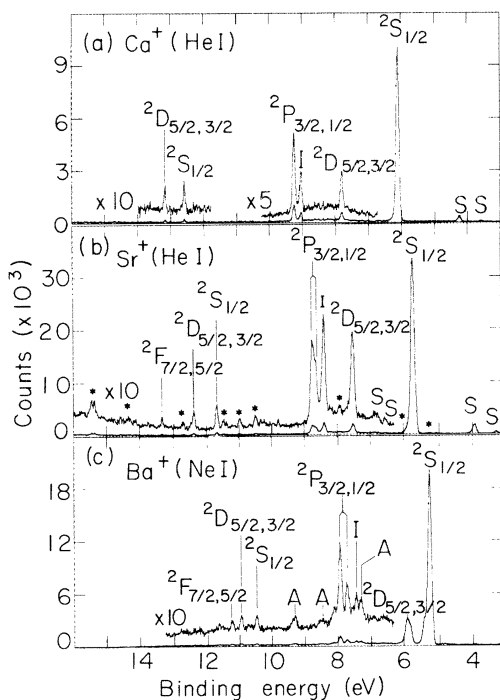


FIG. 1. Photoelectron spectra of (a) Ca (He I radiation, 740 °C); (b) Sr (He I radiation, 650 °C); and (c) Ba (Ne I radiation, 700 °C). Peaks of interest in this work are labeled by spectroscopic symbols. S denotes a peak arising from satellite lines in the incident radiation, and I denotes an inelastic-loss peak. Asterisks denote peaks in the Sr spectrum that arise from autoionizing Ba impurities (see text). Peaks labeled A in the Ba spectrum are tentatively identified as Auger transitions arising from excitation by Ne II radiation.

energies of 7.53, 8.64 (plus 8.73), 11.61, 12.30, and 13.25 eV, corresponding, respectively, to final states ( $4d; ^2D_{3/2,5/2}$ ), ( $5p; ^2P_{1/2,3/2}$ ), ( $6s; ^2S_{1/2}$ ), ( $5d; ^2D_{3/2,5/2}$ ), and ( $4f; ^2F_{5/2,7/2}$ ). The peak designated by I is again an inelastic-loss peak from the transition ( $5s^2 \rightarrow 5s5p; ^1P_1$ ) in neutral Sr. The peaks marked with asterisks (\*) are from transitions in the Ba impurity.

The Ne I spectrum of atomic Ba ( $6s^2; ^1S$ ), Fig. 1(c), shows a main peak at 5.21 eV ( $6s; ^2S_{1/2}$ ) [the most intense Ne I lines actually are a doublet with 0.18-eV separation],<sup>8</sup> and five additional peaks at 5.81 (plus 5.91), 7.70 (plus 7.92), 10.46, 10.92, and 11.20 eV, corresponding, respectively, to ( $5d; ^2D_{3/2,5/2}$ ), ( $6p; ^2P_{1/2,3/2}$ ), ( $7s; ^2S_{1/2}$ ), ( $6d; ^2D_{3/2,5/2}$ ), and ( $4f; ^2F_{5/2,7/2}$ ) final states of Ba. The peak designated by I is an inelastic-loss peak ( $6s^2 \rightarrow 6s6p; ^1P_1$ ) in neutral Ba, and those marked by A's are believed to be Auger lines arising from ionization of core electrons by Ne II radiation.

The He I photoelectron spectra of Zn, Cd, and Hg are shown in Fig. 2. Figure 2 also depicts the  $^2D$  lines of these atoms taken with He II in the same

run. Assignments and derived parameters are tabulated in Table II. The area ratios of the main lines taken at different photon energies are given in Table III. The spectrum of atomic Zn ( $3d^{10}4s^2; ^1S$ ), Fig. 2(a), shows three main peaks at binding energies of 9.39, 17.17, and 17.50 eV corresponding to the Zn<sup>+</sup> final states ( $3s^{10}4s; ^2S_{1/2}$ ), ( $3d^94s^2; ^2D_{3/2}$ ), and ( $3d^94s^2; ^2D_{5/2}$ ), and two additional peaks at 15.40 and 15.51 eV, corresponding to ( $3d^{10}4p; ^2P_{1/2}$ ) and ( $3d^{10}4p; ^2P_{3/2}$ ) final states embedded between  $^2D$  lines excited by the He I  $\beta$  (23.08 eV) radiation. The peak I is an inelastic-loss peak ( $3d^{10}4s^2; -3d^{10}4s4p; ^1P_1$ ). The peaks at 18.6 and 18.8 eV cannot be identified with any known transitions.

The spectrum of Cd ( $4d^{10}5s^2; ^1S$ ), Fig. 2(b), shows, in agreement with our earlier work,<sup>1</sup> two satellites at 14.45 and 14.76 eV, corresponding to ( $4d^{10}5p; ^2P_{1/2}$ ) and ( $4d^{10}5p; ^2P_{3/2}$ ) final states. There is also an inelastic-loss peak (I), near the ( $^2P_{1/2}$ ) line. The statistical accuracy of the present spectrum is much better.

The Hg spectrum Fig. 2(c) shows satellites at 16.83 and 17.96 eV, corresponding to ( $5d^{10}6p; ^2P_{1/2}$ ) and ( $5d^{10}6p; ^2P_{3/2}$ ) final states. These have been reported before by other workers,<sup>3</sup> and are included here for comparison. The line I is again an inelastic-loss peak.

#### IV. DISCUSSION

##### A. Nature of satellite peaks

Recent theoretical analyses<sup>9,10</sup> have been made of the manner in which correlation effects can lead to satellites in photoemission spectra. There are three mechanisms that describe the breakdown of the one-electron picture: initial-state configuration interaction (ISCI), final-ionic-state configuration interaction (FISCI), and continuum-state configuration interaction (CSCI), or inter-channel coupling. FISCI is well known in atoms,<sup>11</sup> molecules,<sup>12</sup> and solids,<sup>13</sup> while ISCI was reported for Hg by Berkowitz *et al.*<sup>3</sup> and by Süzer *et al.* for <sup>1</sup>Cd and <sup>2</sup>Pb.

The distinction among these three mechanisms is not completely unambiguous, because precise statements about configuration interaction can be made only within the context of a particular basis set. In the group-IIA and -IIB elements, however, the FISCI mechanism is expected to be relatively unimportant, because the final ionic states have only one electron outside a closed shell or major subshell (for helium, FISCI could be rigorously excluded<sup>10</sup>). The initial states of these closed-shell atoms possess near-degenerate configurations that are known to mix strongly with the ground state. This phenomenon is termed "internal correlation" by McKoy and Sinanoğlu.<sup>14</sup> In

TABLE I. Observed states of Ca<sup>+</sup>, Sr<sup>+</sup>, and Ba<sup>+</sup>.

Ion	Final state	Apparent relative intensity <sup>a</sup>	Binding energy <sup>a</sup> (eV)	Energy from optical data <sup>b</sup> (eV)
Ca <sup>+</sup>	4s; <sup>2</sup> S <sub>1/2</sub>	100	6.11(2)	6.111
	3d; <sup>2</sup> D <sub>3/2,5/2</sub>	4.5	7.82(2)	7.803; 7.811
	4p; <sup>2</sup> P <sub>1/2,3/2</sub>	10.3	9.24(2)	9.234; 9.262
	5s; <sup>2</sup> S <sub>1/2</sub>	1.6	12.60(2)	12.579
	4d; <sup>2</sup> D <sub>3/2,5/2</sub>	1.5	13.16(2)	13.158; 13.161
Ca <sup>c</sup>	4s4p; <sup>1</sup> P <sub>1</sub>		9.04(2) <sup>d</sup>	9.044 <sup>d</sup>
Sr <sup>+</sup>	5s; <sup>2</sup> S <sub>1/2</sub>	100	5.69(2)	5.692
	4d; <sup>2</sup> D <sub>3/2,5/2</sub>	4.5	7.53(2)	7.497; 7.541
	5p; <sup>2</sup> P <sub>1/2,3/2</sub>	6.5	8.64; 8.73(2)	8.632; 8.732
	6s; <sup>2</sup> S <sub>1/2</sub>	1.0	11.61(2)	11.611
	5d; <sup>2</sup> D <sub>3/2,5/2</sub>	0.6	12.30(2)	12.300; 12.309
4f; <sup>2</sup> F <sub>5/2,7/2</sub>	0.4	13.25(2)	13.250	
Sr <sup>c</sup>	5s5p; <sup>1</sup> P <sub>1</sub>		8.38(2) <sup>d</sup>	8.382 <sup>d</sup>
Ba <sup>+</sup>	6s; <sup>2</sup> S <sub>1/2</sub>	100	5.21(3)	5.211
	5d; <sup>2</sup> D <sub>3/2,5/2</sub>	22.1	5.81; 5.92(3)	5.816; 5.915
	6p; <sup>2</sup> P <sub>1/2,3/2</sub>	1.5; 3.2	7.70; 7.92(3)	7.723; 7.933
	7s; <sup>2</sup> S <sub>1/2</sub>	0.7	10.46(3)	10.463
	6d; <sup>2</sup> D <sub>3/2,5/2</sub>	0.7	10.92(3)	10.908; 10.934
	4f; <sup>2</sup> F <sub>5/2,7/2</sub>	0.5	11.20(3)	11.195; 11.222
Ba <sup>c</sup>	6s6p; <sup>1</sup> P <sub>1</sub>		7.45(3) <sup>d</sup>	7.450 <sup>d</sup>

<sup>a</sup> This work. Xe and N<sub>2</sub> were used for calibration. Areas were corrected for  $\Delta E/E$ ; the Ca and Sr were taken with He I radiation, the Ba with Ne I.

<sup>b</sup> Reference 7.

<sup>c</sup> Inelastic-loss peaks in neutral Ca, Sr, and Ba originate from <sup>2</sup>S<sub>1/2</sub> lines (see text).

<sup>d</sup> Apparent binding energy.

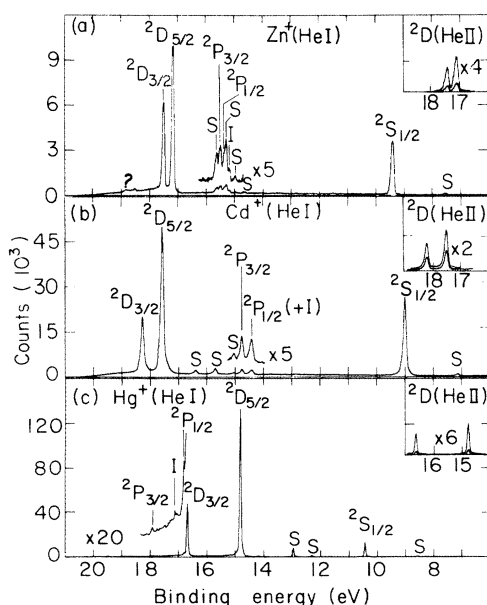


FIG. 2. Photoelectron spectra of Zn, Cd, and Hg, with notation as in Fig. 1. Insets denote He II-excited <sup>2</sup>D lines.

group-IIA elements both the  $np$  and the  $(n-1)d$  shells are empty and low lying, while in Ba the  $4f$  shell is also available for configuration mixing. In group-IIB atoms, the  $(n-1)d$  shell is filled, but the  $np$  shell is expected to mix substantially. We therefore believe that ISCI rather than FISC is dominant in the spectra reported here, and a qualitative interpretation neglecting FISC seems justified.

The importance of interchannel coupling (CSCI) is difficult to evaluate, and it may constitute a sizable correction to the interpretation of our spectra in terms of ISCI alone. In their study of the <sup>2</sup>P satellites in the photoionization of Hg, Berkowitz *et al.*<sup>3</sup> calculated that ~80% of the intensity arose via ISCI. This supports our approach. The other 20% was calculated to arise via “conjugate shakeup,” in which the photon’s angular momentum is transferred to one of the passive electrons. We note that conjugate shakeup can be regarded as a specific configuration interaction that falls under the general category of interchannel coupling. The <sup>2</sup>D and <sup>2</sup>F final states in our spectra could not arise via conjugate shake-

TABLE II. Observed states of Zn<sup>+</sup>, Cd<sup>+</sup>, and Hg<sup>+</sup>.

Ion	Final state	Apparent relative intensity <sup>a</sup>	Binding energy <sup>a</sup> (eV)	Energy from optical data <sup>b</sup> (eV)
Zn <sup>+</sup>	$3d^{10}4s; ^2S_{1/2}$	100	9.39(2)	9.391
	$3d^{10}4p; ^2P_{1/2}$	7	15.40(2)	15.400
	$^2P_{3/2}$	12	15.51(2)	15.509
	$3d^94s^2; ^2D_{5/2}$	611	17.17(2)	17.166
	$^2D_{3/2}$	429	17.50(2)	17.503
Zn <sup>c</sup>	$3d^{10}4s4p; ^1P_1$		15.19(2) <sup>d</sup>	15.187 <sup>d</sup>
Cd <sup>+</sup>	$4d^{10}5s; ^2S_{1/2}$	100	8.99(2)	8.991
	$4d^{10}5p; ^2P_{1/2}$	5	14.45(2)	14.462
	$^2P_{3/2}$	10	14.76(2)	14.770
	$4d^95s^2; ^2D_{5/2}$	622	17.58(2)	17.576
	$^2D_{3/2}$	305	18.27(2)	18.274
Cd <sup>c</sup>	$4d^{10}5s5p; ^1P_1$		14.40(2) <sup>d</sup>	14.401 <sup>d</sup>
Hg <sup>+</sup>	$5d^{10}6s; ^2S_{1/2}$	100	10.43(2)	10.435
	$5d^{10}6p; ^2P_{1/2}$	25	16.83(2)	16.816
	$^2P_{3/2}$	7	17.96(2)	17.947
	$5d^96s^2; ^2D_{5/2}$	1719	14.84(2)	14.837
	$^2D_{3/2}$	781	16.70(2)	16.700
Hg <sup>c</sup>	$5d^{10}6s6p; ^1P_1$		17.13(2)	17.132

<sup>a</sup> This work. Xe and Ar used for calibration. Areas corrected for  $\Delta E/E$ .

<sup>b</sup> Reference 7.

<sup>c</sup> Inelastic-loss peaks in neutral Zn, Cd, and Hg (see text). Originates from  $^2S_{1/2}$  lines.

<sup>d</sup> Apparent binding energy.

up, but CSCI through continuum channels could lead to these states. In general CSCI is expected to be most important near threshold and/or for ions with closely-spaced states of the same symmetry. Thus it should be a good approximation to neglect CSCI in interpreting these satellite

spectra, especially for the lowest-energy ionic states.

Even within the constraint of interpreting the spectra entirely in terms of ISCI, we still do not have enough theoretical information for a complete quantitative interpretation. In particular,

TABLE III. Comparison of experiment with MCHF calculations.

	Calculated mixing coefficients: ratios of the squares of the coefficients normalized to $(ns^2)^a$			Experimentally observed intensities normalized to $ns$ peak <sup>b</sup>		
	$a^2$	$b^2$	$c^2$	$a'^2(ns; ^2S)$	$b'^2(np; ^2P)$	$c'^2(n'd; ^2D)$
Mg: $n = n' = 3$	1.00	0.075	0.0010			
Ca: $n = 4, n' = 3$	1.00	0.087	0.0034	1.00	0.103	0.045
Sr: $n = 5, n' = 4$	1.00	0.085	0.0055	1.00	0.065	0.045
Ba: $n = 6, n'' = 5$	1.00	0.092	0.011	1.00	0.047	0.221

<sup>a</sup> Reference 4.

<sup>b</sup> This work. Observed intensities of satellites. Areas are the total of the spin-orbit doublets (see Sec. IV A).

the relative photoemission cross sections from various subshells are unknown, as in the angular dependence (our spectra were taken in  $90^\circ$  geometry with unpolarized radiation). Our results are set out in the tables to facilitate a more complete interpretation when more theoretical parameters become available. We give below an approximate interpretation in which line intensities are compared directly with ISCI admixture coefficients, neglecting cross-section differences, angular dependences, and FISC and CSCI effects.

The ground states of group-IIA and -IIB atoms can be approximated as

$$\psi(^1S) \cong a(ns^2) + b(np^2) + c(n'd^2) + d(n''f^2) + \dots, \quad (2)$$

with

$$n' = n - 1 \text{ if available, } n'' = n - 2 \text{ if available.}$$

The photoionization spectrum should therefore be dominated by the primary ionic state ( $ns; ^2S$ ), with satellites corresponding to ( $np; ^2P$ ), ( $n'd; ^2D$ ), ( $n''f; ^2F$ ), etc. Within the approximations discussed above, the satellite intensities should vary roughly as  $a^2:b^2:c^2:\dots$ . Kim and Bagus<sup>4</sup> did a multiconfiguration Hartree-Fock (MCHF) calculation to evaluate the generalized oscillator strengths of group-IIA atoms by including ( $np$ )<sup>2</sup> or ( $np$ )<sup>2</sup> and ( $n'd$ )<sup>2</sup> configurations in the ground state. We compare the squares of mixing coefficients  $a^2$ ,  $b^2$ ,  $c^2$ , etc. from their results, with our experimentally observed intensities of the corresponding satellites, in Table III. There is an almost constant value of 9% for the calculated intensities of the ( $np$ )<sup>2</sup> configuration. Experimentally the intensities of the ( $np; ^2P$ ) lines decrease going down the Periodic Table from 10% in Ca and 5% in Ba. This agreement is qualitatively good in view of the experimental accuracy and the assumptions made in the comparison. By contrast, the experimental ( $n'd; ^2D$ ) intensities are much higher than the calculated values and the discrepancy gets worse going down the Periodic Table. For Ba it is 22% experimentally, compared to the calculated 1.1%. This suggests either that the difference between the photoionization cross sections of  $ns$  and  $n'd$  electrons is very large in the comparison or that another mechanism also contributes to the satellite intensities. The other possible contributors are autoionization and interchannel coupling. We have measured the spectrum of Ba using Ar I (11.83 eV) radiation, and found that the relative intensities of the  $5d$  lines remained essentially the same as in the Ne I case. This indicates that the two aforementioned mechanisms are probably not major contributors to the discrepancy, because their contributions are expected to be

strongly dependent on the photon energy. Similar conclusions can be drawn for Ca and Sr, because we observed about the same relative intensities of ( $n'd; ^2D$ ) lines in the He I and Ne I spectra. This leads us to conclude that the differences in photoionization cross sections are too large for such a comparison to be meaningful for the ( $n'd; ^2D$ ) lines. One factor that could account for part of the enhanced intensity of the  $^2D$  lines in the  $2l+1$  multiplicity of the final continuum states. The  $d$  electron would go into  $p$  or  $f$  waves with a total multiplicity of  $3+7=10$ , compared to 3 for the  $s$  electrons, which go into  $p$  waves.

In the spectra of  $\text{Ca}^+$ ,  $\text{Sr}^+$ , and  $\text{Ba}^+$ , a few weaker satellites with relative intensities less than 2% were also detected; they correspond to higher excited states of these ions. Their existence can again be accounted for by ISCI, by interchannel coupling, or by a combination of the two. For the excited  $((n+1)s; ^2S)$  lines, FISC (or shakeup) is also a possible mechanism. Here it is even more difficult to differentiate the individual contributions. We note, however, energy considerations alone give a fairly good indication of how important the ISCI effects on satellites are, while no such *a priori* rule is available for the interchannel coupling effects. Thus the increase of satellite intensities toward lower binding energy is consistent with the ISCI interpretation.

For group-IIB atoms, the satellite intensities of the satellites amount to 20% of the primary peak. Again both ISCI and interchannel coupling can be contributory, and it is difficult to distinguish between them. However, by comparing with Group-IIA atoms, we tend to believe that ISCI is the dominant mechanism. Unfortunately no CI calculations on group-IIB atoms are available for comparison with these spectra.

#### B. Relativistic effects on the branching ratios of spin-orbit components

It is widely recognized that the presence of spin-orbit (SO) coupling can cause the branching ratios of SO components to deviate from the statistical ratios. Recently, Walker *et al.*<sup>15</sup> found the  $^2D_{5/2}/^2D_{3/2}$  branching ratios for Cd and Hg to be significantly greater than the statistical value  $\frac{3}{2}$  for photoemission at 584 Å. These deviations were attributed<sup>15</sup> mainly to two causes, the difference in the initial-state wave functions for  $d_{5/2}$  and  $d_{3/2}$  bound orbitals and the difference in photoelectron kinetic energy. It was further pointed out that the effect of energy difference is important only at lower photon energies, when the photoelectron energy is not too large compared to the SO split-

ting. As the photoelectron energy becomes much larger than the SO splitting, its effect diminishes and the deviation from the statistical ratio will be predominantly due to difference in wave functions. Furthermore, the generalization has been made that if the partial cross section is rising, the ratio of cross sections is greater than statistical, and vice versa.

In Hg,<sup>6</sup> the wavelength dependence of the  ${}^2D_{5/2}/{}^2D_{3/2}$  ratio was observed to follow the generalization. The marked deviation (dropping from 2 to 1.3 for the range  $600 \geq \lambda \geq 200 \text{ \AA}$ ) of the ratio from the statistical is understandable in view of the large SO splitting, and is to be attributed to the difference in the initial-state wave function. In view of this, it is interesting to see how the ratios for Zn and Cd behave, and thus how important are the relativistic effects. We have measured the ratios for Zn, Cd, and Hg using both He I and He II radiation (Table IV). Our results for Hg, after being adjusted for angular dependence using  $\beta$  asymmetry parameters given in Ref. 6, are in good agreement with those reported by Dehmer and Berkowitz,<sup>6</sup> except at 584 Å. The agreement tends to support our expectation that the results for He II radiation are less susceptible to the influence of inelastic loss and charging, and thus are more reliable. Turning to Zn and Cd, in view of the experimental accuracy the  ${}^2D_{5/2}/{}^2D_{3/2}$  branching ratios at both 304 and 256 Å can be regarded as little different from 1.5, in

contrast to Hg. This behavior of the ratio suggests that the relativistic effects in Zn and Cd are too small to cause an appreciable difference in the initial-state wave function, and thus the ratio is around 1.5 at higher photoelectron energy. The deviation of the ratio in Cd at 584 Å is most probably due to the photoelectron energy difference.

In the case of open shells, SO coupling introduces still another relativistic effect on the branching ratio.<sup>3</sup> As the SO coupling gets larger, it may then be more appropriate to use the  $j$ - $j$  coupling scheme, and the component with lower  $J$  value lies lower in energy when the shell is less than half filled. In the  $j$ - $j$  coupling description, as one goes down the series Zn, Cd, and Hg,  $(p_{1/2})^2$  will mix increasingly stronger than the  $(p_{3/2})^2$  configuration with the  $(ns)^2$  primary configuration owing to increasing SO splitting. As a result the observed  ${}^2P_{3/2}/{}^2P_{1/2}$  branching ratio will to a first approximation be given by the ratio of the squares of the corresponding mixing coefficients. Depending upon the magnitude of this relativistic effect, the observed  ${}^2P_{3/2}/{}^2P_{1/2}$  ratio may differ significantly from the statistical value 2 given in the  $L$ - $S$  coupling limit. Experimentally the  ${}^2P_{3/2}/{}^2P_{1/2}$  branching ratio (Table IV) is 1.7 for Zn and 2.0 for Cd, but decreases to a dramatically low value of 0.28 for Hg. This indicates again that relativistic effects are significant in Hg, but small in Zn and Cd, in accord with the conclusion drawn from the  ${}^2D_{5/2}/{}^2D_{3/2}$  ratio. The  ${}^2P_{3/2}/{}^2P_{1/2}$  ratio of 0.28 for Hg is in good agreement with the work of Hotop and Mahr,<sup>16</sup> who measured a value of 0.25 from their high-resolution spectrum of Hg. It is significant to note that the measured ratio is much smaller than the value of 0.8 calculated by the relativistic configuration-interaction method.<sup>3</sup> This large discrepancy is surprising in view of the fact that the relativistic calculation has actually included the conjugate shakeup mechanism, which would be expected to be the major contributor in the interchannel coupling. However, the calculation did not include the effects of the difference in the partial cross sections arising from the differences in the photoelectron kinetic energy and in the initial-state wave functions.

For the alkaline-earth atoms, the experimental resolution did not permit us to resolve the SO doublets (e.g.,  ${}^2D_{5/2,3/2}$ ,  ${}^2P_{3/2,1/2}$ , etc.). In any event, the SO splittings are not large (e.g.,  $6p$  splitting is 0.21 eV for Ba<sup>+</sup> vs 1.13 eV for Hg); thus we do not expect the relativistic effect to be significant. In fact, the branching ratio observed for  $6p$  doublets (Table I) is not much different from the statistical ratio, corroborating our expectation.

TABLE IV. Experimentally observed line intensities for Zn, Cd, and Hg.

$\lambda$ (Å)	State	Area Ratios		
		Zn	Cd	Hg <sup>a</sup>
584	${}^2S_{1/2}$	0.23	0.33	0.13(0.08) (0.025) <sup>b</sup>
	${}^2D_{5/2}$	1.42	2.0	2.20(2.28) (2.00)
	${}^2D_{3/2}$	1.00	1.00	1.00(1.00) (1.00)
304	${}^2S_{1/2}$			0.04(0.03) (0.027)
	${}^2D_{5/2}$	1.46	1.53	1.38(1.36) (1.37)
	${}^2D_{3/2}$	1.00	1.00	1.00(1.00) (1.00)
256	${}^2S_{1/2}$			
	${}^2D_{5/2}$	1.48	1.56	1.32(1.31) (1.32)
	${}^2D_{3/2}$	1.00	1.00	1.00(1.00) (1.00)
243	${}^2S_{1/2}$			
	${}^2D_{5/2}$			1.30 (1.30) <sup>c</sup>
	${}^2D_{3/2}$			1.30 (1.00)

<sup>a</sup> Values in parentheses are branching ratios, where angular dependence is corrected, as was done in Ref. 3.

<sup>b</sup> Values in this column are taken from Ref. 3 for comparison.

<sup>c</sup> Estimated from Fig. 4 of Ref. 3.

## V. CONCLUSIONS

This work has demonstrated the feasibility of doing ultraviolet photoelectron spectroscopic measurements on high-temperature atomic metal vapors up to 750 °C. Satellite lines have now been identified in a total of six group-IIA and -IIB elements. The lines were attributed mainly to initial-state configuration interaction. A complete quantitative interpretation awaits further theoretical progress on cross-section calculations as well as on estimates of the magnitude of final-state and coupled-channel contributions. Espe-

cially after these refinements are made, photoelectron spectroscopy holds promise of becoming a decisive method for studying electron correlation. Finally, intensity ratios for the spin-orbit split components of *p* and *d* shells were found to deviate from statistical value in Hg but not in Cd and Zn, supporting and extending the results of earlier work.

## ACKNOWLEDGMENTS

We are indebted to Geri Richmond and E. Mathias for assistance in taking the spectra of group-IIA elements.

---

\*Work done under the auspices of the U. S. Energy Research and Development Administration.

<sup>1</sup>Ş. Sizer and D. A. Shirley, *J. Chem. Phys.* **61**, 2481 (1974).

<sup>2</sup>Ş. Sizer, M. S. Banna, and D. A. Shirley, *J. Chem. Phys.* **63**, 3473 (1975).

<sup>3</sup>J. Berkowitz, J. L. Dehmer, Y. K. Kim, and J. P. Desclaux, *J. Chem. Phys.* **61**, 2556 (1974).

<sup>4</sup>Y. Y. Kim and P. S. Bagus, *Phys. Rev. A* **8**, 2739 (1973).

<sup>5</sup>H. Hotop and D. Mahr, *J. Phys. B* **8**, L301 (1975); B. Brehm and K. Höfler, *Int. J. Mass Spectrom. Ion Phys.* **17**, 371 (1975).

<sup>6</sup>J. L. Dehmer and J. Berkowitz, *Phys. Rev. A* **10**, 484 (1974).

<sup>7</sup>C. E. Moore, *Atomic Energy Levels*, U. S. Natl. Bur. Stand. Circ. No. 467, (U. S. GPO, Washington, D. C., 1962) Vols. 2 and 3.

<sup>8</sup>J. A. R. Samson, *Techniques of Vacuum Ultraviolet Spectroscopy* (Wiley, New York, 1967).

<sup>9</sup>R. L. Martin and D. A. Shirley, *J. Chem. Phys.* (to

be published).

<sup>10</sup>S. T. Manson, private communication.

<sup>11</sup>D. P. Spears, H. J. Fischeck, and T. A. Carlson, *Phys. Rev. A* **9**, 1603 (1974); F. Wulleumier and M. O. Krause, *Phys. Rev. A* **10**, 242 (1974).

<sup>12</sup>R. N. Dixon and S. E. Hull, *Chem. Phys. Lett.* **3**, 367 (1969); M. Okuda and N. Johathan, *J. Electron Spectrosc. Relat. Phenom.* **3**, 19 (1974); A. W. Potts and T. A. Williams, *ibid.* **3**, 5 (1974); J. C. Lorquet and C. Cadet, *Chem. Phys. Lett.* **3**, 198 (1970).

<sup>13</sup>S. P. Kowalczyk, L. Ley, and R. A. Pollak, F. R. McFeely, and D. A. Shirley, *Phys. Rev. B* **7**, 4009 (1973); C. S. Fadley, D. A. Shirley, A. J. Freeman, P. S. Bagus, and J. V. Mallon, *Phys. Rev. Lett.* **23**, 1397 (1969); A. Rosencwaig, G. K. Wertheim, and H. J. Guggenheim, *ibid.* **27**, 479 (1971).

<sup>14</sup>V. McKoy and D. Sinanoğlu, *J. Chem. Phys.* **41**, 2689 (1964).

<sup>15</sup>T. E. H. Walker, J. Berkowitz, J. L. Dehmer, and J. T. Waber, *Phys. Rev. Lett.* **31**, 678 (1973).

<sup>16</sup>H. Hotop and D. Mahr, private communication.